Forced Shelf Circulation by an Alongshore Wind Band

SHENN-YU CHAO

Oceanographic Center, Nova University, Dania, FL 33004

(Manuscript received 2 March 1981, in final form 3 August 1981)

ABSTRACT

The forced circulation over a continental shelf generated by the alongshore wind stress is studied within the frictional regime. The model alongshore wind stress has a finite extent in the alongshore direction and oscillates monochromatically, resembling a series of anticyclones traveling across the coastline. Both the shelf-wave response and the localized non-wavelike response exist within the wind band. The numerical results show that the interaction of shelf waves with locally wind-forced response generates a large increase in the phase speed within the wind band. Given an alongshore variation in the alongshore wind stress, a right-bounded phase propagation is possible even in the absence of continental shelf waves. Given a reasonable friction currently accepted for the east coast of the United States, the resonance mechanism at the cutoff frequency may not be important, and lower frequency wind events generate larger amplitude continental shelf circulation. By reducing the friction, energy at cutoff frequencies leaks out of the wind band in both directions effectively. It also is shown that non-wavelike response depends only on the local wind stress and is not affected significantly by friction.

1. Introduction

This work was motivated by Brooks' (1979) observation that the phase of the sea level fluctuations in the middle and the south Atlantic Bight tends to propagate in the right-bounded (we call it forward) direction, suggesting that these may be continental shelf waves propagating southward. Brooks' investigation was relatively large scale, spanning an alongshore distance of 1200 km. On a short alongshore scale of 350 km, observations made by Chao and Pietrafesa (1980) along the North Carolina coast suggest that the shelf waters responded to the local wind to a large extent. Continental shelf waves, if they exist, are not observed from these sea level data. These indicate that the sea level fluctuations along the North Carolina coast are largely associated with the forced continental shelf circulation, which behaves quite differently from a free continental shelf wave.

Unless there is a wind stress propagating in the left-bounded (backward) direction, sea level oscillations tend to propagate in the forward direction. From numerous observations, backward propagation of sea level is rather uncommon. For example, during the summer of 1973 the phase of sea level fluctuations off the west coast of the United States propagated northward (forward) consistently over an alongshore distance of 1600 km (Wang and Mooers, 1977). LeBlond and Mysak (1977) gave an extensive review of many observations on this subject.

Observed phase speeds of sea level oscillations are sometimes larger than the phase speeds predicted by the free wave theory. For example, Hamon (1966) observed an average phase speed of 4 m s^{-1} along the entire east Australian coast. Based on a free wave calculation, Robinson (1964) computed a phase speed of 2.5 m s^{-1} for this region, while Buchwald and Adams (1968) obtained a speed of 2.8 m s^{-1}. Off the North Carolina coast, Mysak and Hamon (1969) observed a phase speed 2–4 times larger than the model-predicted value. A coastal tide gage study from the Florida Straits by Brooks and Mooers (1977) also documented anomalously large observed phase speeds.

There are also observations documenting spectral peaks of sea level fluctuations near cutoff frequencies where the group speed of shelf waves is zero (e.g., Cutchin and Smith, 1973; Brooks, 1978), suggesting that the resonant mechanism at cutoff frequencies is important. This certainly is a theoretically sound argument within the limit of inviscid dynamics. One might wonder if the resonant mechanism exists given a realistic amount of friction.

We present a simple numerical model here to address the interaction of barotropic shelf waves with the localized wind-forced response generated by a monochromatic, alongshore wind band. Similar problems were addressed previously by Adams and Buchwald (1969), and later on simplified by Gill and Schumann (1974) in the nondispersive and inviscid limit. They found that in this long wave

0022-3670/81/101325-09$06.25

limit, the forward phase speed for a single mode was increased by a factor of 2 as a result of interaction between long waves and locally generated response.

In this paper we return to this problem and generalize it to the higher-frequency and frictional regime. The objectives of the present work are to study the following:

1) the localized (non-wavelike) response and its interaction with shelf waves over the continental shelves;

2) the resonant mechanism at the cutoff frequencies; and

3) the frictional effect on the continental shelf circulation.

2. Formulation

Consider a homogeneous fluid rotating about its vertical axis with a constant angular frequency $f/2$. The coastline is along the x axis, with positive x pointing southward (forward). The y axis points offshore. A rigid lid is assumed at the water surface. The shelf profile, assumed to be uniform in the alongshore direction, is exponential:

$$h(y) = \begin{cases} \exp[2.3 \times 10^{-2}(y - 100)] \text{ km} \\ \qquad y < 100 \text{ km} \\ 1 \text{ km} \quad 100 \text{ km} < y < 200 \text{ km}, \end{cases} \tag{1}$$

where all numerical values are in units of kilometers. We also put a vertical wall along $y = 200$ km to isolate the shelf water from the oceanic interior. The dispersion diagram for the first two shelf wave modes for this topography is shown in Fig. 1.

The linear governing equations of motion are

$$\frac{\partial u}{\partial t} - fv = -p_x + \frac{\tau^{(x)}}{h} - \frac{ru}{h}, \tag{2}$$

$$\frac{\partial v}{\partial t} + fu = -p_y \qquad - \frac{rv}{h}, \tag{3}$$

$$\frac{\partial}{\partial x}(hu) + \frac{\partial}{\partial y}(hv) = 0, \tag{4}$$

where (u, v) are depth-averaged velocities in the (x, y) directions, respectively, $\tau^{(x)}$ is the alongshore wind stress, and r is a linear bottom friction.

We assume that the alongshore wind stress $\tau^{(x)}$ varies only in the alongshore direction and vanishes outside a finite domain $0 \leq x \leq L$. The wind stress

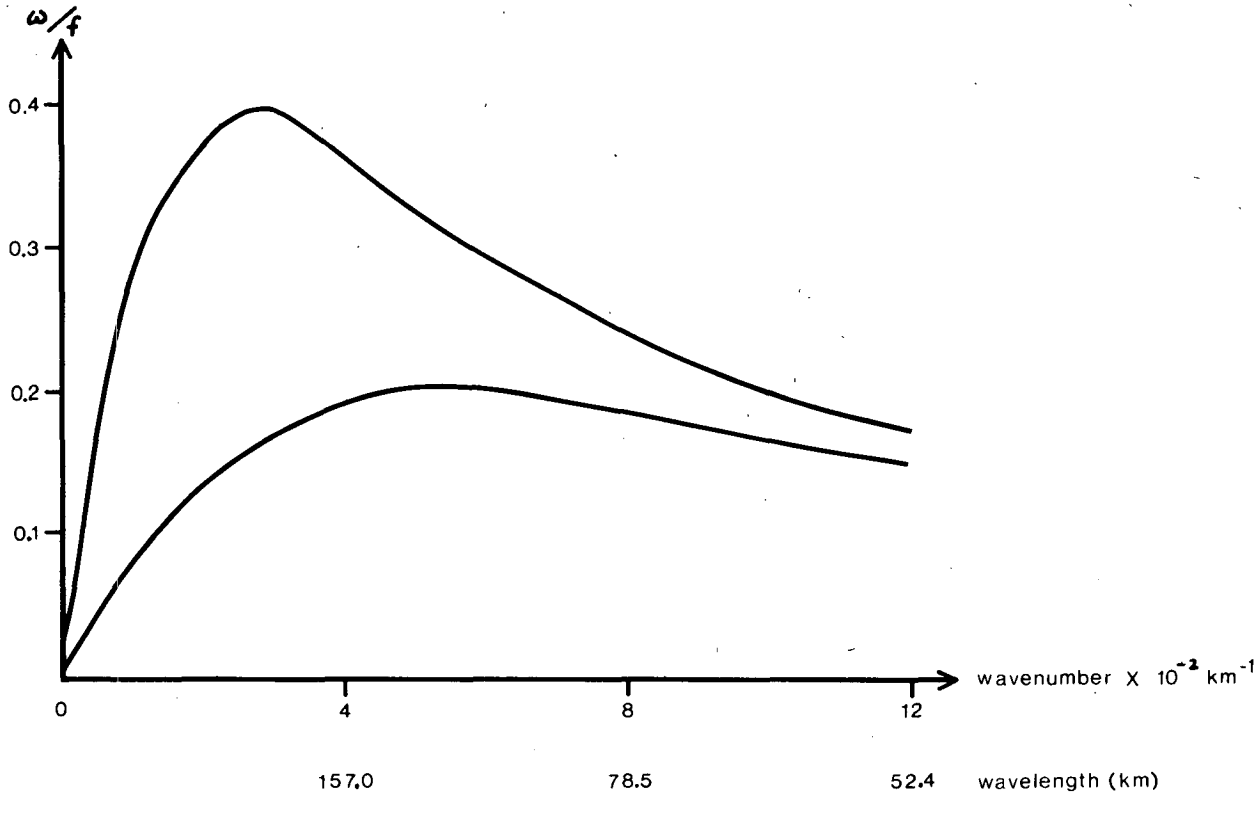

FIG. 1. The dispersion relation of the first two shelf-wave modes of the exponential depth profile given in Eq. (1).

distribution is given by

$$\tau^{(x)} = \begin{cases} 0 & x \leq 0 \\ \dfrac{\tau_0}{M} x e^{i\omega t} & 0 \leq x \leq M \\ \tau_0 e^{i\omega t} & M \leq x \leq N, \\ \dfrac{\tau_0}{N-L}(x-L)e^{i\omega t} & N \leq x \leq L \\ 0 & x \geq L \end{cases} \quad (5)$$

where $\tau_0 = -1$ dyn cm^{-2}, and M, N, L are 250, 750 and 1000 km, respectively. The model wind stress given in Eq. (5) is fairly realistic in some regions. For example, the major weather features in Australia and the eastern United States consist of a series of anticyclones traveling across the coastline.

By defining a mass transport streamfunction ψ such that

$$hu = \psi_y, \quad hv = -\psi_x, \quad (6)$$

a governing equation in ψ can be derived from Eqs. (2) and (3) as

$$\frac{\partial}{\partial t'}\nabla^2\psi - \left(\frac{r}{h} + \frac{\partial}{\partial t'}\right)\frac{hy}{h}\psi_y - f\frac{hy}{h}\psi_x = -\frac{hy}{h}\tau^{(x)}, \quad (7)$$

where

$$\frac{\partial}{\partial t'} \equiv \frac{\partial}{\partial t} + \frac{r}{h},$$

$$\nabla^2 \equiv \frac{\partial^2}{\partial x^2} + \frac{\partial^2}{\partial y^2}.$$

The boundary conditions imposed on Eq. (7) are

(i) no normal flux across vertical walls, i.e.,

$$\psi = 0 \quad \text{at} \quad y = 0, 200 \text{ km}, \quad (8)$$

(ii)

$$\psi_x = 0 \quad \text{as} \quad x \to \pm\infty. \quad (9)$$

The governing equation (7) along with boundary conditions (8) and (9) are solved by the numerical scheme of Lindzen and Kuo (1969). The time dependence ($e^{i\omega t}$) can be factored out from Eq. (7). Boundary conditions (9) are imposed at finite but large distances instead of infinity. The accuracy of the numerical results is insured if the solutions are insensitive to the alongshore boundaries imposed. This is achieved provided that the alongshore boundaries are 2000 km or more away from the wind band. In fact, most of the forced shelf waves decay to zero before they even reach the boundary. We also vary the location where the offshore vertical wall is placed. The results show that solutions over the shelf and slope region are insensitive to the offshore location of the vertical wall.

3. Numerical results

Throughout the model studies the Coriolis parameter f is taken to be 0.89×10^{-4} s^{-1}. A typical friction coefficient r for the east coast of the United States is $r = 0.1$ cm s^{-1} (Csanady, 1978). We will take this typical friction and a relatively inviscid case ($r = 0.005$ cm s^{-1}) for the sake of comparison. Numerical solutions are expressed in terms of the amplitude and the phase. If $A(x, y, t) = B(x, y)e^{i\omega t + i\phi(x,y)}$, the real quantities B and ϕ are the amplitude and the phase of A, respectively. If ϕ is positive (negative), A leads (lags) the wind stress by an angle ϕ.

Fig. 2 shows the amplitude and the phase of the mass transport streamfunction ψ for $\omega = 0.3f$ and $r = 0.1$ cm s^{-1}. At $\omega = 0.3f$ only the first-mode shelf wave is possible. The amplitude of the streamfunction shows that the energy propagates predominantly in the forward direction, consistent with the result that large-scale wind stress favors long-wave generation in the nondispersive limit (Gill and Shumann, 1974). The phase pattern shows that throughout the channel, the phase propagates in the forward direction. The long-wave forward of the wind band has a wavelength of ~700 km, while shorter waves backward of the wind band have a wavelength of ~120 km. Over the shelf and slope region, the nearshore phase generally leads the offshore phase, consistent with the theory of Brink and Allen (1978). An exception exists at the backward edge of the wind band ($0 \leq x \leq 250$ km), where the nearshore phase lags the offshore phase instead. This phenomenon has no relation to the backward leaking of the short wave energy, as the nearshore phase leads the offshore phase even in the short-wave dominated region (Fig. 2). We will demonstrate that this is associated with the nonwavelike response in the next section.

Fig. 3 shows the amplitude of alongshore transport (hu) along the coast for various frequencies and $r = 0.1$ cm s^{-1}. At all frequencies below the cutoff frequency ($\omega = \omega_c = 0.395f$), energy leaks in the forward direction. In the nondispersive limit ($\omega \leq 0.2f$), the amplitude favors the forward edge of the wind band, while at higher frequencies the amplitude favors the backward edge of the wind band instead. At the cutoff frequency, the wavelength becomes shorter and there is a double peak structure within the wind band. This double-peak structure is caused by the short wavelength of the free wave component and has no relation to the resonant effect. This is dealt with in Section 4.

Resonance at the cutoff frequency does not show up in Fig. 3, due to the effect of large friction.

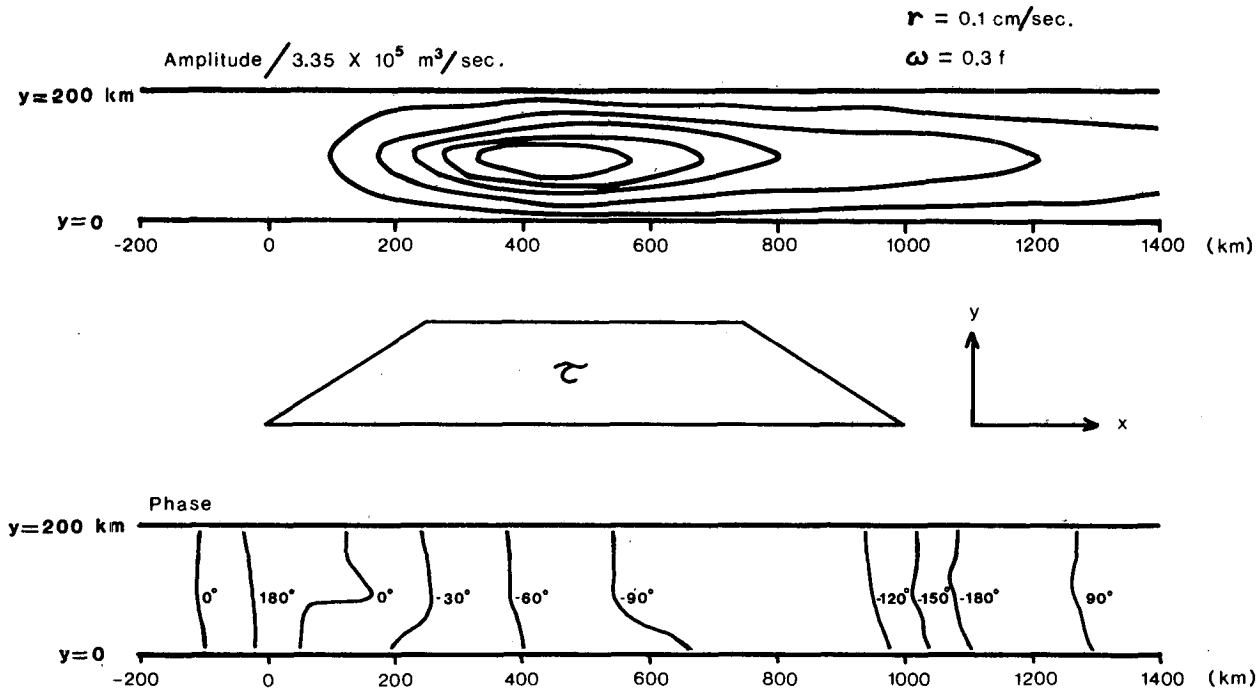

FIG. 2. The amplitude and phase of the mass transport streamfunction for $\omega = 0.3f$, $r = 0.1$ cm s^{-1}. The wind-stress location and the coordinate system are also shown.

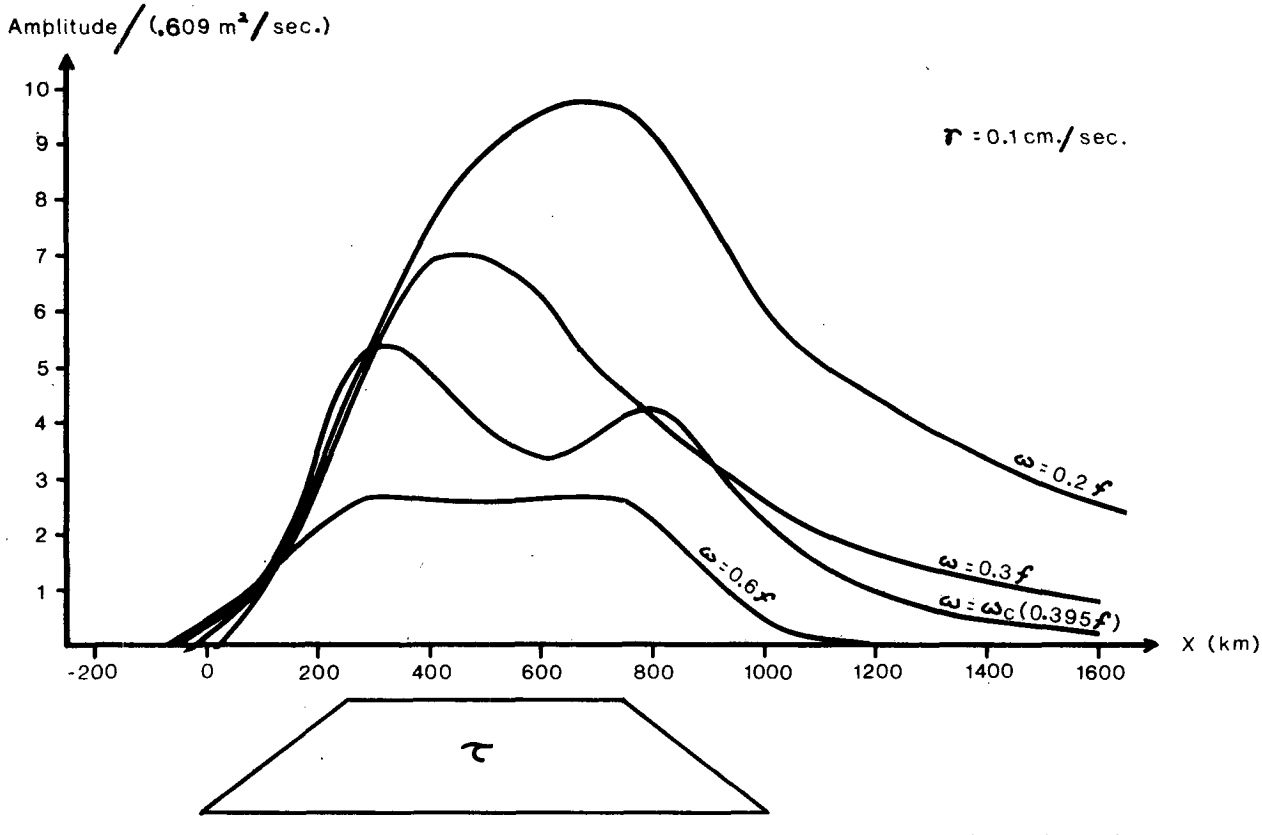

FIG. 3. The amplitude of coastal alongshore transport ($y = 0$) for various frequencies and $r = 0.1$ cm s^{-1}.

Beyond the cutoff frequency, where no shelf wave is allowed, the amplitude of the coastal alongshore flow is almost a mirror image of the wind-stress pattern. This is expected, because a localized response cannot communicate with a neighboring point in the absence of waves. We also notice that in this frictional case the amplitude tends to decrease as frequency increases. This is consistent with the one-dimensional model of Chao and Pietrafesa (1980), who showed that low-frequency wind events are more effective in generating coastal flow.

Fig. 4 shows the phase of alongshore transport at $y = 0$ for various frequencies and $r = 0.1$ cm s^{-1}. The slope of this figure gives the local wavenumber, from which one can compute the phase speed. At $\omega = 0.2f$ and forward of the wind band, a long wave of wavelength ~1200 km travels forward with a phase speed of 294 km day^{-1}, in agreement with the value predicted by the dispersion curve (Fig. 1). Backward-leaking shelf-wave energy with wavelength of ~50 km outside of the wind band are of negligible amplitudes (Fig. 3) and hence are not shown in Fig. 4. The average phase speed within the wind band between $x = 250$ km and $x = 750$ km is five times larger than the phase speed outside and forward of the wind band. There is a slight local backward phase propagation within the forward edge of the wind band (600 km $\leq x \leq$ 800 km) at $\omega = 0.3f$. This phenomenon is more noticeable as the wavelength becomes shorter. At the cut-off frequency ($\omega = 0.395f$), there is a stronger backward phase propagation within the wind band. At $\omega = 0.6f$, where shelf waves are absent, there is no phase difference between $x = 250$ km and $x = 750$ km, where the wind stress is uniform. However, at the two edges of the wind band, alongshore variation of the wind stress brings about a phase propagation in the forward direction. The phase difference between the backward and forward edges of the wind band is ~180°.

Similar computations are carried out for the case of smaller friction ($r = 0.005$ cm s^{-1}). Fig. 5 shows the amplitude of the alongshore transport along $y = 0$. Below the cutoff frequency, the amplitude is larger than in the case of greater friction ($r = 0.1$ cm s^{-1}). Beyond the cutoff frequency, the amplitudes are nearly identical. Thus the frictional effect has little to do with the localized (non-wavelike) response. Near the cutoff frequency, double-peak structure still exists within the wind band. Outside the wind band, the amplitude is rather sensitive to the frequency. At $\omega = 0.39f$, forward energy leaking is more intense, while at $\omega = 0.4f$ backward energy leaking is stronger. It should be noted here that backward and outside of the wind band, energy leaks backward in the direction of group speed while the phase propagation is forward. One

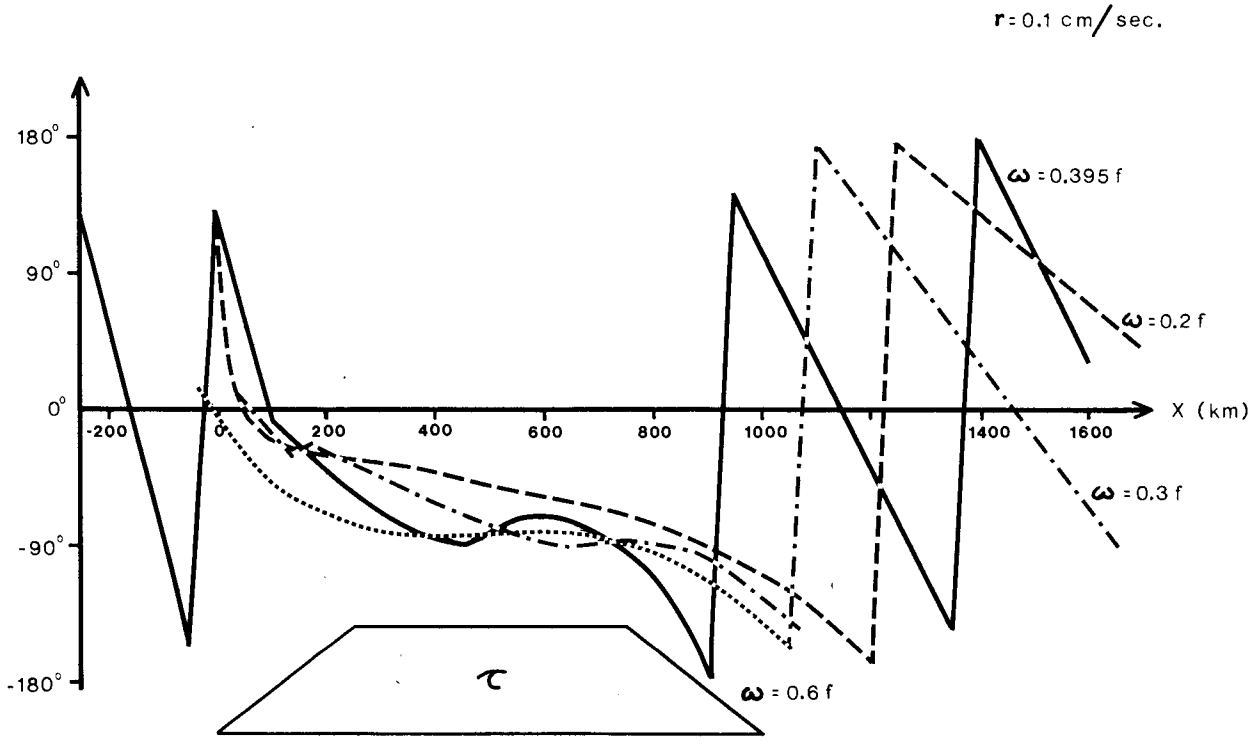

FIG. 4. The phase of coastal alongshore transport ($y = 0$) for various frequencies and $r = 0.1$ cm s^{-1}.

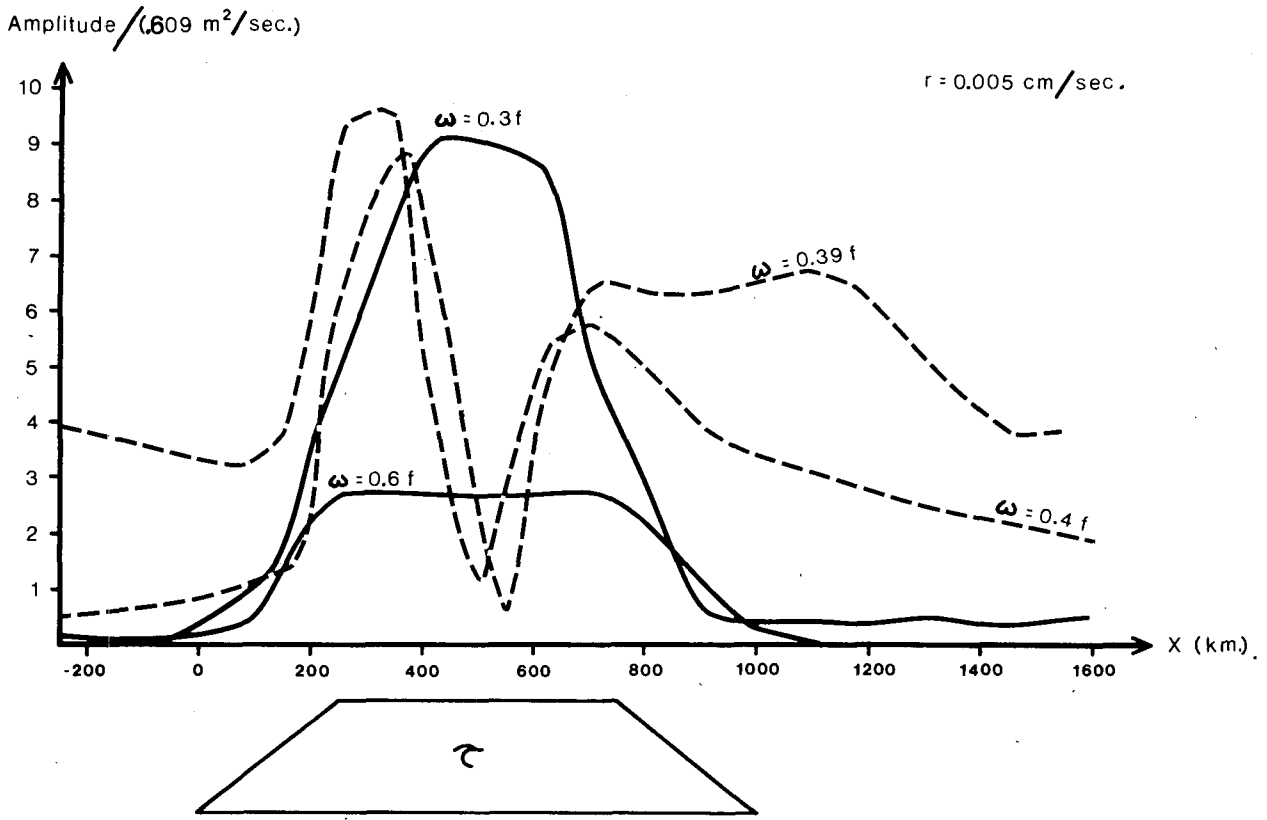

FIG. 5. As in Fig. 3 except $r = 0.005$ cm s^{-1}.

also notices that the resonance mechanism at the cutoff frequency begins to show up in the case of smaller friction. Amplitudes near the cutoff frequency are comparable to the low-frequency response. Also, energy leaks out of the wind band more effectively than with large friction (Fig. 3).

Fig. 6 shows the phase of the alongshore transport for the case $r = 0.005$ cm s^{-1}. At $\omega = 0.6f$ the phase is nearly identical to the $r = 0.1$ cm s^{-1} case (Fig. 4). The backward phase propagation within the wind band at and below the cutoff frequency becomes more intense in the case of smaller friction. From Figs. 4 and 6, we also notice that the phase tends to drop from 0 to $-180°$ from the backward edge to the forward edge of the wind stress.

4. Discussion

We have studied the forced circulation over a continental shelf generated by a monochromatic, alongshore wind band in the frictional regime. Given a reasonable amount of friction, one need not consider a radiation condition at the alongshore boundaries, provided that the boundary conditions are applied sufficiently away from the wind band. Alternatively, one could consider an inviscid problem under which the radiation boundary conditions utilized by Wang (1980) would apply. However, the currently accepted value for friction off the eastern United States coast is $r = 0.1$ cm s^{-1}, under which the solution does behave quite differently from the inviscid case.

The increase in phase speed within the wind band is directly related to observations and deserves further comment. Mysak and Hamon (1969) noted that the observed southward coastal sea level phase lags along North Carolina were several times smaller than they were predicted to be, a result they suggested could be explained by interferences of local and nonlocal disturbances. Brooks (1978) suggested a similar interference mechanism between locally and nonlocally forced oscillations. Our theoretical results support their interpretation.

The physics behind this phenomenon is as follows. Suppose that a traveling shelf wave and a locally forced oscillation are both present and of equal magnitude; the superposition of both components gives

$$(1 + e^{ikx})e^{-i\omega t} = 2\cos\left(\frac{k}{2}x\right)e^{i(kx/2-\omega t)}, \quad (10)$$

so that the phase speed is increased by a factor of 2 locally. This is actually the result of the long wave limit as obtained by Gill and Schumann (1974). Our

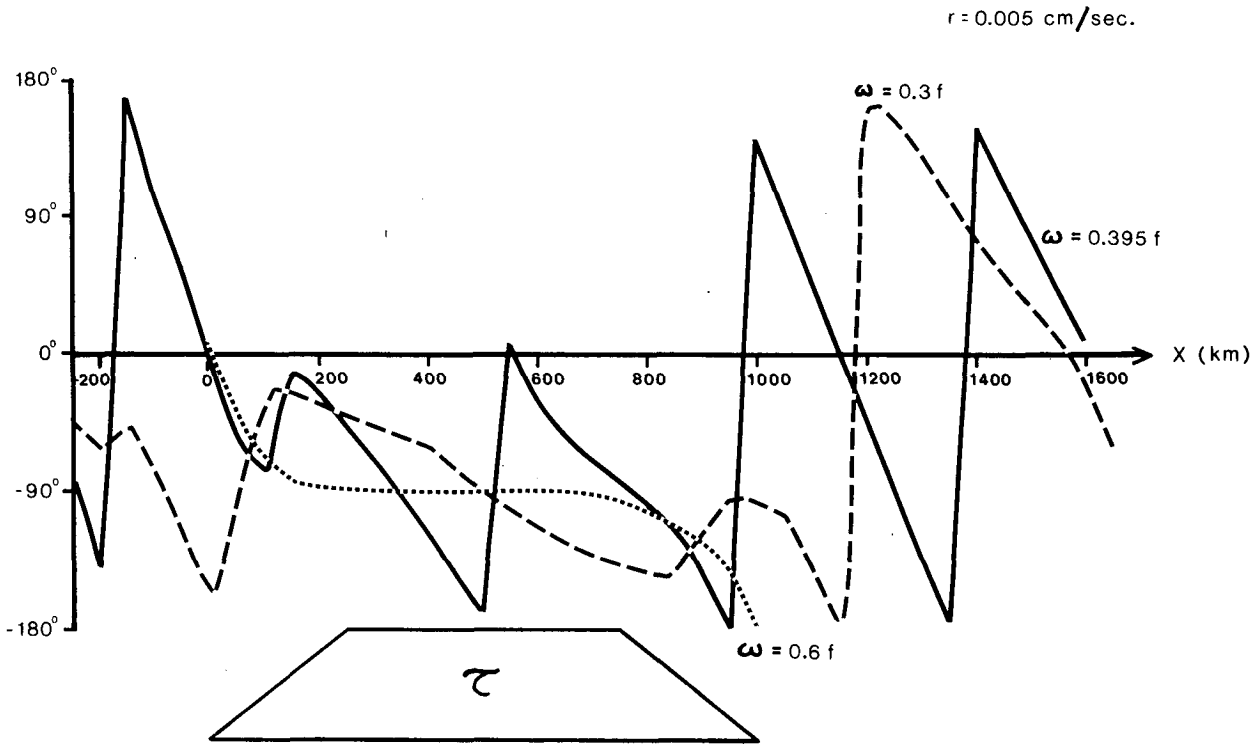

FIG. 6. As in Fig. 4 except $r = 0.005$ cm s^{-1}.

situation is more complex than the argument given, but essentially a reduction in wavelength further increases the phase speed within the wind band. If the wavelength of the free wave is too short compared to the length of the wind band (L), $\cos[(k/2)x]$ in Eq. (10) changes sign within the wind band and there is a 180° phase jump along with a local nodal point in amplitude. This actually occurs in the relatively inviscid case for $\omega = 0.395f$ (Figs. 5 and 6). An increase in friction reduces the wavelike component while keeping the non-wavelike component unchanged. As a consequence, the 180° phase jump in the relatively inviscid case becomes a weak phase propagation in the backward direction in the case of greater friction (Fig. 4); and the nodal point in Fig. 5 becomes a local amplitude minimum in Fig. 3 within the wind band.

The nearshore phase lags the offshore phase over the continental shelf near the backward edge of the wind band (Fig. 2, $0 \leq x \leq 250$ km), in contrast to the theory of Brink and Allen (1978). This phenomenon occurs at all frequencies, although only $\omega = 0.3f$ is shown in Fig. 2. The backward edge of the wind band is the region where long-wave components are small. Therefore, the phenomenon must be related to the localized non-wavelike response. To illustrate this, consider a high frequency of $\omega = 0.6f$ response. Fig. 7 shows the phase of alongshore transport across the shelf at $x = 125$, 500 and 875 km for $\omega = 0.6f$. The nearshore phase lags the offshore phase at $x = 125$ km (Fig. 7). The theory of Brink and Allen (1978), however, agrees with our calculation for $x = 500$ and 875 km.

The resonance mechanism at the gravest mode cutoff frequency is wiped out by friction unless $r \leq 0.005$ cm s^{-1}. If the bottom friction (r) equals 0.1 cm s^{-1} as suggested by Csanady (1978), the continental shelf circulation off the east coast of the United States will be dominated by the frictional effects and the inviscid dynamics such as resonance will not be important. However, since the bottom friction is difficult to estimate accurately, the possibility of resonance as suggested by Brooks (1978) cannot be ruled out. More careful observations are needed to resolve this issue. Instead of choosing one possibility over the other, our model results quantify their differences.

The phase of shelf waves propagates in the direction of phase speed, while the shelf wave energy propagates in the direction of group speed. At low frequencies ($\omega \ll f$) the wind forcing favors forward-propagating long waves. At higher frequencies shelf waves become highly dispersive and the energy of shelf waves can propagate either way. These waveguide characteristics are reflected in our numerical results (Fig. 3) that the backward edge of the wind band is favored at higher frequencies. In the steady-state solution of Csanady (1978), a large sea level amplitude is found near the

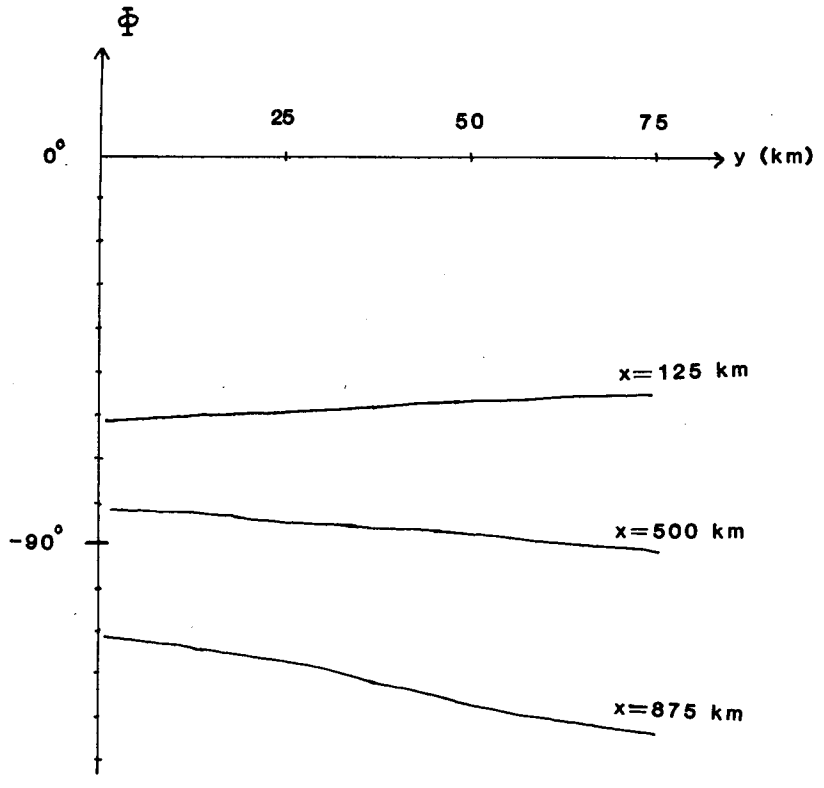

FIG. 7. The phase of the alongshore transport across the shelf at x = 125, 500 and 875 km for $\omega = 0.6f$.

forward edge of the wind band and there is an upward slope in the direction of the alongshore wind. His result is consistent with our low-frequency behavior.

The assumption of a periodic wind stress is adopted in this paper because a majority of coastal sea level data interpretations is done in the frequency domain. In the real world the wind is not finely tuned to a single frequency. However, given a sufficiently long time series of coastal sea level data and assuming that the wind forced response is fairly linear, a periodic wind-stress model can sometimes yield information closely related to observations interpreted in the frequency domain, information which cannot otherwise be easily extracted from a more sophisticated model. The large increase in phase speed within the wind band, as often observed in tide gage data, is an example. There is no direct analogy between the periodic wind-stress model considered here and the impulsively started wind-stress model (e.g., Allen, 1976), since the frequency information does not enter directly into the initial value problem. However, short time behavior ($t \ll 1$) of an initial value approach is consisted of our high-frequency solutions while the large time behavior ($t \gg 1$) is consisted of our low-frequency ($\omega \ll f$) solutions (Lighthill, 1967). The numerical experiments of Suginohara (1974) support this statement. Suginohara (1974) studied the spin-up of a two-layer, coastal ocean by an impulsively started alongshore wind band. Shortly after the onset of the winds ($t < 2$ days) the nearshore streamline pattern is almost a mirror image of the wind band, consistent with our high-frequency ($\omega > \omega_c$) behavior (Fig. 3). From 2 to 6 days the maximum amplitude response propagates from the backward edge to the forward edge of the wind band, consistent with our results that the location of the maximum alongshore flow moves forward as the frequency decreases (Fig. 3).

5. Conclusions

1) The interaction of long shelf waves and locally wind-forced response brings about a large increase in phase speed, as compared to the phase speed of free shelf waves. The increase is larger as the wavelength becomes shorter. If the wavelength is too short compared to the scale of the wind band, a backward propagation of phase speed will be observed within the wind band.

2) Above the critical frequency where no free wave is possible, forward propagation of phase speed exists if there is an alongshore variation in

alongshore wind stress. The phase variations over both edges of the wind stress, where the wind varies alongshore, are 90° each, which add up to a 180° phase difference across the whole wind band.

3) The nonwavelike (localized) response is not significantly affected by friction.

4) In the nondispersive limit, the amplitudes for the streamfunction and the alongshore flow favor the forward edge of the wind band, while at higher frequencies the backward edge is favored. At higher frequencies where the wavelength of the long wave becomes shorter than a multiple peak structure for the amplitude of ψ and u is observed within the wind band. Above the cutoff frequency, localized non-wavelike response is trapped within the wind band and depends only on the strength of local wind stress.

5) Defining the maximum friction as $R_{MAX} = r/h(y = 0)$, the resonance mechanism becomes important when $(R_{MAX}/\omega_c) < O(10^{-2})$. For $R_{MAX} \gg 0.01\omega_c$, the resonance mechanism is not important and lower frequency wind events always generate higher amplitude circulation. For a lower friction where the resonance is important, energy effectively leaks out of the wind band in both forward and backward directions.

6) Backward and outside of the wind band, energy is propagating backward while the phase is propagating forward.

7) At regions where low-frequency long shelf waves are important, nearshore phase leads offshore phase, consistent with Brink and Allen (1978).

Acknowledgments. The author is indebted to Dr. Pijush Kundu for carefully reading the manuscript and offering valuable comments. He also thanks Dr. Julian McCreary for discussions concerning the physics of this subject. Drs. W.-S. Chuang and R. E. Hall also offered some interesting suggestions. This work was supported by NASA/Goddard Space Flight Center under Contract NAS5-26051 and partially by the National Science Foundation under Grant OCE-8023790.

REFERENCES

Adams, J. K., and V. T. Buchwald, 1969: The generation of continental shelf waves. *J. Fluid Mech.*, **35**, 815–826.

Allen, J. S., 1976: Some aspects of the forced wave response of stratified coastal regions. *J. Phys. Oceanogr.*, **6**, 113–119.

Brink, K. H., and J. S. Allen, 1978: On the effect of bottom friction on barotropic motion over the continental shelf. *J. Phys. Oceanogr.*, **8**, 919–922.

Brooks, D. A., 1978: Subtidal sea level fluctuations and their relation to atmospheric forcing along the North Carolina coast. *J. Phys. Oceanogr.*, **8**, 481–493.

——, 1979: Coupling of the Middle and South Atlantic bights by forced sea level oscillations. *J. Phys. Oceanogr.*, **9**, 1304–1311.

——, and C. N. K. Mooers, 1977: Wind-forced continental shelf waves in the Florida Current. *J. Geophys. Res.*, **82**, 2569–2576.

Buchwald, V. T., and J. K. Adams, 1968: The propagation of continental shelf waves. *Proc. Roy. Soc. London*, **A305**, 235–250.

Chao, S.-Y., and L. J. Pietrafesa, 1980: The subtidal response of sea level to atmospheric forcing in the Carolina capes. *J. Phys. Oceanogr.*, **10**, 1246–1255.

Csanady, G. T., 1978: The arrested topographic wave. *J. Phys. Oceanogr.*, **8**, 47–62.

Cutchin, D. L., and R. L. Smith, 1973: Continental shelf waves: Low frequency variations in sea level and currents over the Oregon continental shelf. *J. Phys. Oceanogr.*, **3**, 73–82.

Gill, A. E. and E. H. Schumann, 1974: The generation of long shelf waves by the wind. *J. Phys. Oceanogr.*, **4**, 83–90.

Hamon, B. V., 1966: Continental shelf waves and the effects of atmospheric pressure and wind stress on sea level. *J. Geophys. Res.*, **71**, 2883–2893.

LeBlond, P. H., and L. A. Mysak, 1977: Trapped coastal waves and their role in shelf dynamics. *The Sea*, Vol. 6, E. Goldberg, I. McCave, J. O'Brien and J. Steele, Eds., Wiley-Interscience, 459–495.

Lighthill, M. J., 1967: On waves generated in dispersive systems by travelling forcing effects, with applications to the dynamics of rotating fluids. *J. Fluid Mech.*, **27**, 725–752.

Lindzen, R. S., and H. L. Kuo, 1969: A reliable method for the numerical integration of a large class of ordinary and partial differential equations. *Mon. Wea. Rev.*, **97**, 732–734.

Mysak, L. A., and B. V. Hamon, 1969: Low-frequency sea level behavior and continental shelf waves off North Carolina. *J. Geophys. Res.*, **74**, 1397–1405.

Robinson, A. R., 1964: Continental shelf waves and the response of sea level to weather systems. *J. Geophys. Res.*, **69**, 367–368.

Suginohara, N., 1974: Onset of coastal upwelling in a two-layer ocean by wind stress with alongshore variation. *J. Oceanogr. Soc. Japan*, **30**, 23–33.

Wang, D.-P., 1980: Diffraction of continental shelf waves by irregular alongshore geometry. *J. Phys. Oceanogr.*, **10**, 1187–1199.

——, and C. N. K. Mooers, 1977: Long coastal-trapped waves off the west coast of the United States, Summer 1973. *J. Phys. Oceanogr.*, **7**, 856–864.